Journal of South American Earth Sciences 62 (2015) 70–79

Contents lists available at ScienceDirect

Journal of South American Earth Sciences

journal homepage: www.elsevier.com/locate/jsames

Optimization of the *in-situ* U–Pb age dating method via LA-Quadrupole-ICP-MS with applications to the timing of U–Zr–Mo mineralization in the Poços de Caldas Alkaline Complex, SE Brazil

Lynthener Bianca Takenaka, Cristiano Lana*, Ricardo Scholz, Herminio Arias Nalini Jr., Adriana Tropia de Abreu

Departamento de Geologia, Universidade Federal de Ouro Preto, Morro do Cruzeiro, Campus, Ouro Preto, MG 35400000, Brazil

ARTICLE INFO

Article history:
Received 19 November 2014
Accepted 29 April 2015
Available online 14 May 2015

Keywords:
LA-ICP-MS
Poços de Caldas alkaline complex
Zircon
U–Pb method

ABSTRACT

The high spatial resolution of the LA-ICP-MS systems allows rapid extraction of vital isotopic information from individual growth zones of minerals. This paper describes in detail the optimization of a relatively inexpensive LA-ICP-MS system consisting of a UV 213 Laser Ablation and a Quadrupole ICP-MS. The results of optimization take into account laser energy, beam diameter, frequency and ICP-MS gas conditions. The optimized conditions were tested for precision and accuracy on a number of well-characterized zircons, commonly used as primary and secondary quality control standards. The acquisition of the U–Pb data is carried out in automated mode (pre-set points) for up to 12 h/day with only minimal operator presence. Individual U–Pb zircon analysis lasts 80 s. The 2σ uncertainties of the standards ranged between 1.4 and 8.2%, and overall their relative deviations ranged from 0.02 to 0.87%. The results are comparable to techniques that use more complex and time-consuming approaches such as LA-MC-ICP-MS and ion-microprobe. We have applied this method to obtain ages of numerous granitoid rocks from the Southern São Francisco Craton and a well-known Archean granitoid of the Kaapvaal Craton, South Africa. We furthermore provide the first results of U–Pb age dating of U–Zr–Mo mineralization in the Poços de Caldas Alkaline Complex, SE Brazil, with a U–Pb age of 85 ± 3 Ma for zircon-bearing hydrothermal veins.

1. Introduction

Laser Ablation system (LA) attached to Inductively Coupled Plasma Mass Spectrometer (ICP-MS) is a relatively simple and affordable combination of instruments that is capable of *in situ* isotope measurements with extremely low detection limits (Fryer et al., 1993). In geochronology, LA-ICP-MS systems are adequate because of sensitivity, high spatial resolution and higher rates of material transference during analysis. Recent advances in gas/solid state laser ablation and in ICP-MS sensitivity has allowed determination of important isotopes (*e.g.*, Hf-, B-, Sr-, Nd-, Pb-) and trace element data from individual growth zones of various minerals such as zircon, monazite, titanite, apatite and tourmaline (*e.g.*, Kinny et al., 1991; Hinton and Upton, 1991; Thirlwall and Walder, 1995; Rubato et al., 2001; Storey et al., 2006; Darlin et al., 2012; Sarkar et al., 2014). Improvements in the through put rates of ICP-MS systems and intelligent automation of laser ablation instruments has allowed acquisition of large datasets in relatively short analytical sections. On the other hand, less sensitive systems such as Quadrupole ICP-MS (Q-ICP-MS) coupled to 213 (or 266)-nm solid-state lasers have to be systematically optimized, in order to avoid recurring problems such as low sensitivity and high elemental fractionation.

The wide dynamic range of Quadrupole-ICP-MS systems permits U–Pb isotopic and trace element analysis of narrow growth zones from a number of minerals such as zircon, monazite and titanite (Jeffries et al., 1998, 2003; Jackson et al., 2004; Storey et al., 2006). Several studies have demonstrated the accuracy and precision of such instruments for U–Pb geochronology (Jackson et al., 2004; Storey et al., 2006) but information about tuning/optimization/data reduction protocols is often scarce. In this paper, we describe the technique and show how a full optimization of the LA-Q-ICP-MS provided optimum results at the end of one year. We

* Corresponding author. Tel.: +55 31 31 98483538.
E-mail address: cristianodeclana@gmail.com (C. Lana).

http://dx.doi.org/10.1016/j.jsames.2015.04.007
0895-9811/

noted that the slightest modifications in the system can result in higher counts (especially for the less abundant masses like ^{204}(Pb + Hg), ^{202}Hg and ^{207}Pb), prevent high oxide formation (ThO << 1%) and produce low elemental fractionation. After systematic normalization against external standards, the system can give ages with high accuracy and acceptable analytical errors. The methodology was tested using five well-characterized zircon standards and a number of magmatic zircons from well-known granitoids in Brazil and South Africa.

As an application to our system, we attempted to estimate the timing of fluid circulation and Zr–U–Mo mineralization in the Poços de Caldas (PC) Alkaline Complex, one of the largest alkaline intrusions in South America (Fig. 1). We provide 34 *in situ* U–Pb analysis from samples of the eastern portion of the PC alkaline complex. These samples came from supergene-enriched deposits of zircon and caldasites located a few kilometers west of the *Osamu Utsumi* uranium mine. Late-stage alkaline fluid activity affected the main body of phonolites and tinguaites and reflects the timing of U–Zr–Mo mineralization in the PC complex. The samples yielded abundant, largely translucent zircons that gave highly concordant and Pb-common free isotopic (U–Pb) ages.

2. Instrumentation and data acquisition

LA-Q-ICP-MS analyses were carried out in an Agilent 7700x mass spectrometer coupled to a laser system LUV213 (New Wave Research/Merchantek, Nd: YAG). The Agilent 7700x ICP-MS is configured for routine analysis with very low concentrations of elements (0.1–2% relative standard deviations), providing sufficient counts on masses such as ^{202}Hg, ^{204}Pb + ^{204}Hg and ^{207}Pb for U–Pb applications in minerals like zircon, monazite and titanite (Lana et al., 2010a,b). The software packages of the Laser Ablation unit and ICP-MS are synchronized via a trigger cable in order to automate the analytical procedure. Individual analyses are produced in

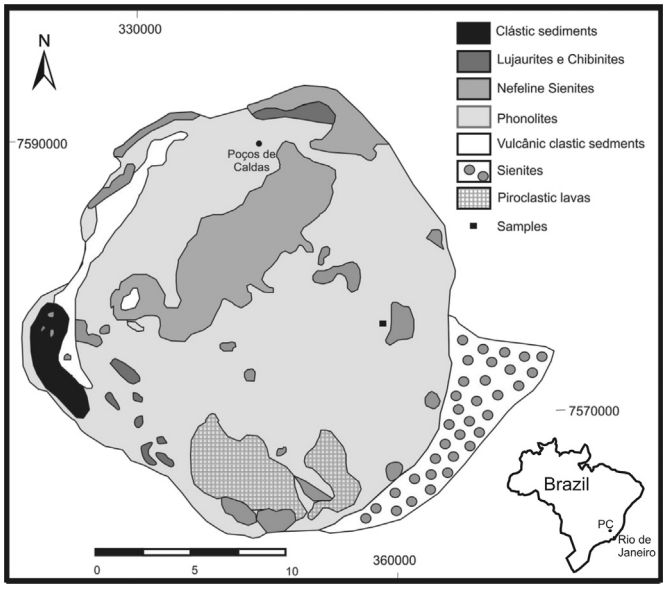

Fig. 1. Geological map of the Poços de Caldas alkaline complex (PC) in SE Brazil. The geology of the complex includes volcanic (breccia, tuff and agglomerate), effusive and hypabyssal (phonolite and tinguaite, respectively), and plutonic (mainly foyaite) rocks in the massif (Fraenkel et al., 1985; Ulbrich and Ulbrich, 1992). Ulbrich and Ulbrich (1992) described a range of rock types that were sequentially emplaced in the following order: 1-tinguaites, 2-phonolites and 3-syenites, and the last basic to ultrabasic volcanic rocks and dikes (sometimes associated with carbonatite occurrences). An early volcanism involving olivine nephelinites, phonolite lavas and volcanoclastics gave way to a caldera subsidence and nepheline syenite intrusions forming minor ring dykes and circular structures (Ellert, 1959).

less than a minute, and a minimum of 40–50 individual dates can be acquired per hour. The analyses are performed keeping all parameters constant (from laser and ICP-MS) for standards and samples throughout the run. The laser is kept always focused, thus reducing any shifts of the laser beam during ablation. The operating conditions of ICP-MS and laser are specified in Table 1.

Standard and sample mounts are placed in a tear-drop shaped sample chamber that was customized at the University of Stellenbosch (Lana et al., 2013; Romano et al., 2013) (Fig. 2). It has two compartments: one of 1 cm-diameter for standard mounts and one of 2.5 cm-diameter for sample mounts (Fig. 2a). In the path between the ablation cell and ICP-MS, the commonly used Y-tube was replaced by a gas mixer (Squid) in the form of a splitter, with ten PTFE tubes of 3 mm diameter and 80 cm in length (Fig. 2b) for better homogenization of the mixtures. The Squid keeps wash out time short and produces a strikingly smooth signal that is perfect for counting statistics (it eliminates the noise) and consequently gives better averaged signal counts.

The integration times used are 40 ms for ^{207}Pb, 15 ms to ^{206}Pb and 10 ms to ^{29}Si, ^{202}Hg, ^{204}(Pb + Hg), ^{208}Pb, ^{232}Th and ^{238}U, with a total scan of the masses occurring in 60 s (20 s background/40 s ablation). The relevant isotopic ratios ^{207}Pb/^{206}Pb, ^{208}Pb/^{206}Pb, ^{208}Pb/^{232}Th, ^{206}Pb/^{238}U and ^{207}Pb/^{235}U (^{235}U is calculated from counts of ^{238}U by natural abundant reason ^{235}U = ^{238}U/137.88) were calculated by the data reduction program Glitter (Van Achterbergh et al., 2001). Background values are measured (20 s) at the beginning of each analysis.

The initial data reduction is done on line via the software Glitter (GEMOC Laser ICP-MS Total Trace Element Reduction), which provides an interactive environment for analytic selection of background and sample signals besides enabling a fast, real-time and online data reduction (Van Achterbergh et al., 2001; Jackson et al., 2004). The program calculates the significant isotopic ratios (^{207}Pb/^{206}Pb, ^{208}Pb/^{232}Th, ^{206}Pb/^{238}U and ^{207}Pb/^{235}U) which are displayed in time-resolved mode. For our laser system, isotopic ratios generated during the first 5 s of each analysis were discarded. The integration window for the remainder of each analysis is chosen so as to exclude signal segments that were related to inclusions, zones of Pb loss (*e.g.*, fractures), high common Pb or inheritance. Mass bias and drift corrections are based on sets of measured standard ratios that bracket sets of 7–10 analysis of

Table 1
Operating conditions of the LA-Quadrupole-ICP-MS system.

ICP-MS	Agilent 7700x
Mass analyzer	Quadrupole
RF Power (W)	1550
Sampler cone	Ni; 1.0 mm
Skimmer cone	Ni; 0.4 mm
Sampling depth (cm)	5
Plasma gas (L min^{-1})	15
Auxiliary gas (L min^{-1})	1.2
Optional gas (L min^{-1})	1
Carrier gas (L min^{-1})	1.00–1.10
Dwell times (ms)	40, 15, 10, 10, 10,10, 10
ThO^+/Th^+ (%)	<0.5
Isotopes (*m*/*z*)	^{207}Pb, ^{206}Pb, ^{208}Pb, ^{232}Th, ^{238}U, ^{29}Si, ^{202}Hg, ^{204}Pb + Hg
Laser	New Wave UV 213
Wavelength (nm)	213
Frequency (Hz)	10
Fluency (J/cm^2)	10
Energy (%)	50
Beam type	*Spot*
Beam diameter (μm)	30–40
Ablation time (s)	40–50

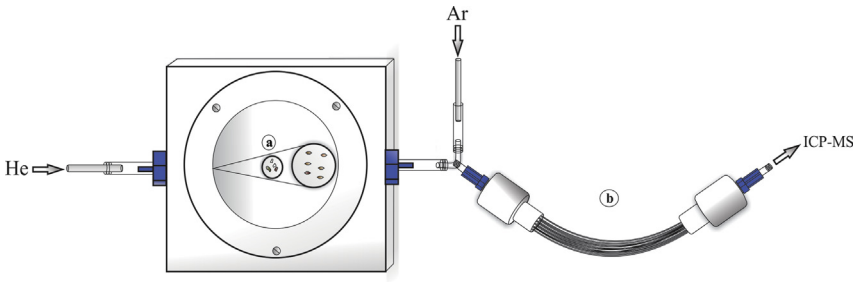

Fig. 2. Sketch of the cell for standards and sample mounts, and the mixing gas system. Note that the cell (a) has a tear drop shape to maximize gas flow and washout. Helium is used for transport of the material and is mixed with Ar after the sample cell for better ionization in the ICP-MS. The gas mixer (b) is essential for homogenization of the sample and gases before it enters in the ICP-MS. The cell is a modified prototype from that designed by the British Geological Survey, in Nottingham (*e.g.*, Bleiner and Günther, 2001; Horstwood et al., 2003).

unknowns. The measured standard ratios are interpolated through a linear regression and the obtained correction factor is applied to the bracketed unknowns. Common Pb corrections are done using the interference and background-corrected ^{204}Pb signal in combination with the Pb model composition of Stacey and Kramers (1975). This is done offline with an in-house excel spreadsheet that takes all mass-bias and drift corrected counts exported from Glitter. Relative uncertainties of the $^{206}Pb/^{207}Pb$ and $^{206}Pb/^{238}U$ ratios combines the external reproducibility of the primary standard with the within-run uncertainties in the quadrature. A further 1% uncertainty (1σ) is assigned to the measured TIMS values of the isotope ratios for the standard and propagated through the analysis error. The $^{207}Pb/^{235}U$ ratio is derived from the normalized and error propagated $^{207}Pb/^{206}Pb$ and $^{206}Pb/^{238}U$ ratios assuming a $^{238}U/^{235}U$ natural abundance ratio of 137.88, and the uncertainty is derived by quadratic addition of the propagated uncertainties of both ($^{207}Pb/^{206}Pb$ and $^{206}Pb/^{238}U$) ratios. We note that for more than 80% of the analysis, the ^{204}Pb counts were often too low (10–30 cps) and the $^{206}Pb/^{204}Pb$ ratios are too high for any significant common Pb correction.

3. Samples and quality control standards

In this study the precision (on errors) and accuracy (for validation of results) were monitored through alternating measurements between the primary GJ-1 standard zircon and several secondary (quality control) standards (zircons Plešovice, M127, BB9 and 91500). Our GJ-1 standard zircon (Jackson et al., 2004; Elhlou et al., 2006) is a gem-quality yellowish crystal with no apparent zoning in cathodoluminescence. Previous U–Pb TIMS dating of this zircon gave and intercept age of 608.5 ± 0.3 Ma (Jackson et al., 2004). The Plešovice standard comprises round to well-shaped short prismatic crystals of approximately 0.1 cm in length. The concordant ID-TIMS age of 337.17 ± 0.18 Ma (Sláma et al., 2008) is conventionally used as the accepted age of this standard. The BB9 zircon comes from a secondary placer deposit in the Sri Lankan Highland Complex (Santos et al., 2014). The crystal is light purple, transparent and shows no internal fracture or significant inclusion that can be observed microscopically. It records a TIMS of 562 ± 1.4 Ma (Santos et al., 2014). The M127 is a homogeneous zircon crystal from Sri Lanka with a TIMS age of 526.42 ± 1.9 Ma ($^{207}Pb/^{206}Pb$) (Nasdala, 2007; Nasdala et al., 2008). The 91500 zircon from Lake Ontario, Canada (Wiedenbeck et al., 1995), is marked by a dark red color flat faces, well-defined edges and no visible inclusion. Previous characterizations provided U–Pb ages by ID-TIMS of 1062.4 ± 0.8 Ma for the $^{207}Pb/^{206}Pb$ ratio and 1065.4 ± 0.6 Ma for the $^{206}Pb/^{238}U$ (Wiedenbeck et al., 1995).

Four Palaeoproterozoic and Archaean granitoid samples were used to evaluate the ability of the instrument to date zircons much older (>2000 Ma) than natural standards (300–600 Ma) used for calibration. The chosen granitoids – previously dated by TIMS – are the Kaap Valley Pluton from the Kaap Vaal Craton (South Africa) and the Samanbaia, Moeda and Alto Maranhão granitoids from the São Francisco Craton (Brazil). The Kaap Valley is a regionally extensive Archean pluton (Robb et al., 1983; Anhaeusser and Robb, 1983), which was dated by Kamo and Davis (1994) at 3227 ± 1 Ma. Less precise ages of 3226 ± 14 Ma and 3229 ± 5 Ma were obtained by Armstrong et al. (1990) (SHRIMP) and Tegtmeyer and Kroner (1987) (single grain evaporation). The Samambaia tonalite records crystallization age of 2780 ± 3 Ma (Machado et al., 1996). The Moeda granodiorite was dated at 2721 Ma by Machado et al. (1992) and Romano et al. (2013) whereas the Alto Maranhão pluton is a tonalite intrusion with a TIMS age of 2124 ± 1 Ma (Noce et al., 1998).

Zircons from the Poços de Caldas complex (SE Brazil; Fig. 1) were analyzed here to obtain information on the age of U–Zr–Mo mineralization. The complex comprises a 33 km-diameter round chimney of alkaline intrusions, with a surface extent of about 800 km^2 and estimated depth of 10–12 km (Fig. 1) (Ulbrich and Ulbrich, 1992). Several samples of a hydrothermally altered phonolite were collected in the eastern portion of the complex, in a deposit named Morro do Taquarí at approximately 6 km northeast from the *Osamu Utsumi* uranium mine (Fig. 1). The interaction between the country rocks and hydrothermal fluids led to crystallization of large crystals of zircon in a baddeleyite-rich microcrystalline groundmass (Fig. 3). These hydrothermal systems are found within large alteration zones of the phonolite, which are observed in and around U–Zr–Mo mines. The outcrops are heavily altered due to supergene enrichment, and the exposures were limited to boulders of the dominant phonolite, that covers more than 60% of the main alkaline complex. The samples consist of a brown cryptocrystalline groundmass with a number of zircon-filled cavities. The groundmass is a Zr rich amorphous phase riddled with baddeleyite microcrystals (Fig. 3).

4. Results

4.1. Optimization

Parameters such as laser beam diameter, ablation time, frequency and extra parts such as the low volume cell, gas splitters and homogenizers were tested in order to obtain the best results with higher counts, precision and accuracy. Tests with 10 Hz laser frequency, 20 and 30 μm-wide beam and 40 s ablation time gave well-shaped 17 and 25 μm-diameter craters respectively and very uniform/stable analytical signals, but undesirable low counts (Condition A – Table 2). Keeping the same gas conditions, but changing the beam to 40 μm-wide, the system produced 33 μm-wide flat craters, stable analytical signal and precise ages (described below) with nearly double counting statistics than the previous condition (Condition B Table 2). The precision of the

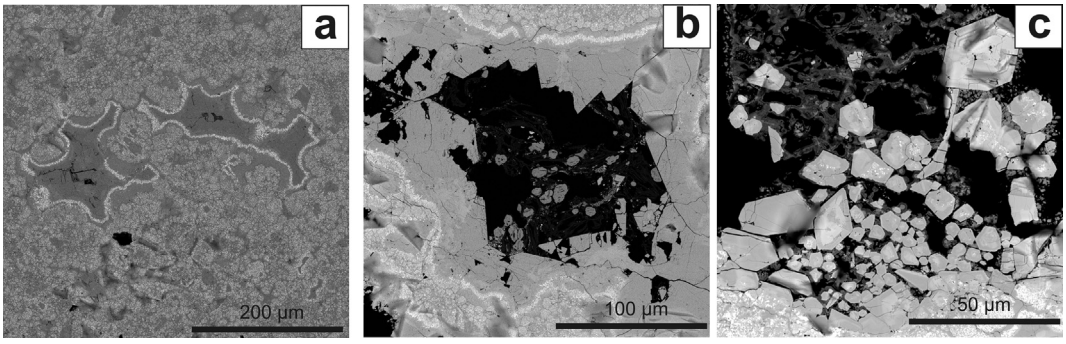

Fig. 3. a) Electron microscope image (backscattered image) showing the main rock composition with cryptocrystalline rock mass and a number of hydrothermal cavities. Bright spots in the groundmass are baddeleyite crystals b) Detail of one hydrothermal cavity showing well faceted zircon crystals crystallized during hydrothermal alteration. The zircons are surrounded by the baddeleyite bearing groundmass. c) Detailed images of zircons from a large 200 µm wide cavity.

$^{207}Pb/^{206}Pb$ ratios increased substantially once the dwell time of the ^{207}Pb mass was modified from 30 ns to 40 ns (Table 2). Tests with 10 Hz frequency, 30 µm-wide beam, and higher ablation times of 50 s, yielded a stable signal but some elemental fractionation affected reproducibility of accepted ages from standards. Moreover, the counts were not satisfactorily high for the purpose of this study. The problem with this last condition is that each individual analysis takes too long, making it difficult to keep a strong stable signal, without significant down-whole fractionation. Tests carried out at 5 Hz, 40 s, and beams of 30 µm and 40 µm, provided very satisfactory analytical signal but with higher analytical errors due to low counts per second of the ^{207}Pb mass. The measured counts per second were 3–4 times lower than those performed in previous conditions A and B.

Table 2 shows results of several runs on the GJ1 zircon for conditions A (30 micron beam) and B (40 micron beam). In both conditions, the instrument gave accurate results within 1% of the accepted age of the GJ1 standard. However, the combination of signal stability, low fractionation (larger crater size) and increased 40 ns dwell time for mass ^{207}Pb (condition B) resulted in much higher precision on all ratios, particularly for the $^{207}Pb/^{206}Pb$ ratio. The errors of the $^{207}Pb/^{206}Pb$ apparent ages in condition B are 30–40 % lower than those of condition A (Table 2). Condition B was proven ideal (giving the Quadrupole performances) for Archean zircons, as the increase in hole size from 30 µm to 40 µm resulted in higher counts, primarily for masses ^{207}Pb and ^{206}Pb (Table 2).

4.2. Zircon standards

The precision (on errors) and accuracy (for validation of results) of the LA-ICP-MS system were monitored through alternating measurements between the primary GJ-1 standard zircon and several secondary standards (zircons Plešovice, M127, BB9 and 91500). Table 3 shows all Concordia ages obtained from sessions 1 to 20 (see also electronic supplement). The compiled results for GJ 1 show Concordia ages ranging from 607 ± 4 Ma to 610.1 ± 3.8 Ma (with deviations from the accepted age ranging from 0 to 0.35) (Table 2; Fig. 4a), fairly consistent with the TIMS intercept age of 607 Ma. The $^{206}Pb/^{238}U$ weighted mean from 746 points gave an age of 608.7 ± 0.47 Ma. The relative deviations for individual ratios were 0.1–3.0% ($^{207}Pb/^{206}Pb$), 0.04–2.8% ($^{206}Pb/^{238}U$) and 0.4–1.9% ($^{207}Pb/^{235}U$). Our Plesovice zircon (sessions 1 to 20 of Table 3; Fig. 4b; electronic supplement) gave Concordia ages ranging from 337 ± 1.6 Ma to 340 ± 1.3 Ma and a $^{206}Pb/^{238}U$ weighted mean of 337.6 ± 0.4 Ma (303 points). Deviations from the accepted value ranged from 0.02 to 0.35%. The relative deviations for individual ratios were 0.4–6.6% ($^{207}Pb/^{206}Pb$), 0.15–2.7% ($^{206}Pb/^{238}U$) and 0.2–2.42% ($^{207}Pb/^{235}U$). Zircon BB9 (sessions 1 through 6 of Table 3; Fig. 4c) gave a range of Concordia ages from 558 ± 2.4 Ma to 566 ± 4.2 Ma and 2σ uncertainties between 2.4 and 4.7%. The $^{206}Pb/^{238}U$ weighted mean from 59 points gave an age of 560.8 ± 1.5 Ma. The relative deviations for individual ratios are 0.03–1.7% ($^{206}Pb/^{238}U$) and 0.2–1.7% ($^{207}Pb/^{235}U$). The analytical sessions for M127 (sessions 1 to 13 of Table 3; Fig. 4d; electronic supplement) yielded Concordia ages ranging from 520 ± 3.5 to 528 ± 3.2 Ma and 2σ uncertainties between 1.4 and 4.3 %. Relative deviations for the individual ratios were 0.19–3.2% ($^{207}Pb/^{206}Pb$), 0.1–1.0% ($^{206}Pb/^{238}U$) and 0.11 to 3.31 ($^{207}Pb/^{235}U$) %. The $^{206}Pb/^{238}U$ weighted mean from 179 points gave an age of 525 ± 0.82 Ma. The calculated Concordia ages for zircon 91500 (sessions 1 to 10 of Table 3; Fig. 4e; electronic supplement) range from 1062 ± 5.1 Ma and 1070 ± 6.5 Ma. Relative deviations for the individual ratios were 0.04–0.41% ($^{206}Pb/^{238}U$), 0.02–0.77% ($^{207}Pb/^{235}U$) and 0.06–2.22% ($^{207}Pb/^{206}Pb$). The $^{206}Pb/^{238}U$ weighted mean from 107 points gave an age of 1064.9 ± 2.2 Ma.

4.3. Natural rock samples

Samples of the Kaap Valley pluton were analyzed in two separate runs. The first round provided an upper intercept age of 3227.9 ± 4.6 Ma and a lower intercept age of 498 ± 270 Ma (MSWD = 0.58) (Fig. 5a). The subsequent run provided an upper intercept age of 3229.4 ± 5.1 Ma and a lower intercept age of 461 ± 210 Ma (MSWD = 1.5) (Fig. 5b). The average ages calculated for the $^{206}Pb/^{238}U$ and $^{207}Pb/^{235}U$ ratios were 3199 ± 14 Ma and 3216 ± 6.1 Ma, 3225 ± 18 Ma and 3228 ± 7.6 Ma, and the mean ages of $^{207}Pb/^{206}Pb$ ratio were 3227 ± 7 Ma and 3229 ± 11 Ma, respectively.

Zircon ages from the Samambaia Tonalite and Moeda Granodiorite were obtained in the same run. Zircons from the Samambaia tonalite were pink to purple, fairly transparent and maked by well defined oscilatory zoning. 32 analyses from these zircons gave concordant points with mean ages of 2785 ± 12 Ma ($^{207}Pb/^{206}Pb$), 2777 ± 14 Ma ($^{206}Pb/^{238}U$) and 2781.5 ± 6.9 Ma ($^{207}Pb/^{235}U$). The same analysis gave a Concordia age of 2782.1 ± 3.7 Ma (Fig. 5c). Most zircons found in the Moeda granodiorite were milky or white and fairly discordant. Only about 20% of the concentrate was sufficient transparent for U–Pb LA-ICP-MS dating. The analyses on the most transparent crystals gave an upper intercept age of 2730.5 ± 6.9 Ma and a lower intercept age of 609 ± 160 Ma (MSWD = 2.2) (Fig. 5d). Average mean ages were found to be 2729 ± 10 Ma for the $^{207}Pb/^{206}Pb$ ratio, 2727 ± 13 Ma for the $^{206}Pb/^{238}U$ ratio and 2728 ± 6.1 Ma for the $^{207}Pb/^{235}U$ ratio.

Table 2
Compilation of runs on standard GJ1 highlighting reproducibility and precision of distinct beam sizes (30 m and 40 um).

Name	U238[a]	Pb207[a]	#	$^{207}Pb/^{206}Pb$[b]			$^{206}Pb/^{238}U$[b]			$^{207}Pb/^{235}U$[b]			$^{207}Pb/^{206}Pb$			$^{206}Pb/^{238}U$			$^{207}Pb/^{235}U$		
	(CPS)	(CPS)		Ratio	2σ (%)	Stdev	Ratio	2σ (%)	Stdev	Ratio	2σ (%)	Stdev	Age[c]	2σ[d]	Stdev[e]	Age	2σ	Stdev	Age	2σ	Stdev
30 micron beam diameter																					
clana42 30 um	34191	2017	20	0.060488	3.60	0.000366	0.099291	3.00	0.000518	0.82819	5.0	0.004739	621	90	13.05	610	16	3.03	613	23	2.62
clana37 30 um	27681	1400	17	0.060229	3.81	0.000567	0.099216	2.77	0.000754	0.82443	4.6	0.007093	612	82	20.28	610	16	4.41	611	22	3.94
clana 35 30 um	24769	2081	19	0.060137	3.60	0.000494	0.098096	2.75	0.000865	0.81281	4.5	0.007039	608	78	17.68	603	16	5.08	604	21	3.95
clana42a30 um	14765	1648	20	0.060459	4.19	0.000366	0.099291	2.70	0.000518	0.82819	5.0	0.004739	621	90	13.05	610	16	3.03	613	23	2.62
clana37 30 um	22980	1410	17	0.060229	4.00	0.000567	0.099285	3.00	0.000754	0.82443	5.0	0.007093	612	82	20.28	610	16	4.41	611	22	3.94
clana51 30 um	19876	1670	24	0.060068	3.07	0.000595	0.099254	2.37	0.001321	0.82185	3.9	0.010566	606	66	21.30	610	14	7.74	609	18	5.86
dlana51	43969	2987	11	0.059936	2.77	0.000645	0.099066	2.46	0.000628	0.81835	3.7	0.005253	601	60	23.45	609	14	3.69	607	17	2.93
A	39809	2699	16	0.060049	2.80	0.00058	0.099586	2.44	0.00094	0.82437	3.7	0.009235	605	61	20.93	612	14	5.51	610	17	5.12
40 micron beam diameter																					
Clana40 40 um	46740	3129	14	0.060206	2.29	0.00068	0.099494	2.76	0.001216	0.82574	3.04	0.006583	611	49	24.42	611	12	7.12	611	14	3.65
7741	55670	3091	21	0.060215	2.03	0.00051	0.099366	1.93	0.001183	0.824919	2.80	0.0105	611	44	18.33	611	11	6.93	611	13	5.85
astd10	41290	3009	9	0.060076	2.50	0.000553	0.099872	2.25	0.000947	0.82725	3.37	0.014276	606	54	19.83	614	13	5.51	612	16	7.93
7470p27f	43908	2980	21	0.060167	2.40	0.001012	0.098955	2.35	0.001965	0.82067	3.36	0.018494	619	52	35.52	608	14	11.52	608	15.5	10.33
7470p27d	30989	2708	18	0.060219	2.42	0.000944	0.099116	2.16	0.001877	0.82262	3.24	0.015535	611	51	33.79	609	13	11.02	609	14.97	8.65
padrao GJ-1	40989	3298	9	0.060076	2.50	0.000553	0.099872	2.25	0.000947	0.82725	3.37	0.014276	606	54	19.83	614	13	5.51	612	15.58	7.93
7470p27d	43090	2908	18	0.060219	2.42	0.000944	0.099116	2.16	0.001877	0.82262	3.24	0.015535	611	51	33.79	609	13	11.02	609	14.97	8.65
7470p27f	52009	3590	21	0.060167	2.40	0.001012	0.098955	2.35	0.001965	0.82067	3.36	0.018494	619	52	35.52	608	14	11.52	608	15.5	10.33
astd10	49990	3908	9	0.060076	2.50	0.000553	0.099872	2.25	0.000947	0.82725	3.37	0.014276	606	54	19.83	614	13	5.51	612	15.58	7.93
7741	37898	2876	21	0.060215	2.03	0.00051	0.099366	1.93	0.001183	0.82492	2.80	0.0105	611	44	18.33	611	11	6.93	611	12.92	5.85
7741a	39800	2989	24	0.059889	2.29	0.000843	0.098711	2.25	0.002093	0.815	3.22	0.020716	599	50	30.40	607	13	12.31	605	14.75	11.70
7742b	44563	3098	21	0.06022	2.20	0.000639	0.099125	2.18	0.000868	0.82294	3.10	0.008009	611	48	23.11	609	13	5.08	610	14.29	4.45

[a] Within-run background-corrected mean ^{207}Pb signal in counts per second [cps].
[b] Corrected for mass-bias by normalizing to reference zircon and common Pb using the model Pb composition of Stacey and Kramers (1975). $^{207}Pb/^{235}U$ calculated using $(^{207}Pb/^{206}Pb)/(^{238}U/^{206}Pb.1/137.88)$.
[c] Average of apparent ages in a single run.
[d] Mean of the error propagated − standard deviation of all (n) analyses within a run.
[e] Standard deviation of apparent ages in a single run.

Table 3
Analytical sessions with Concordia ages obtained for the zircon standards in LA-Quadrupole-ICP-MS system, their 2σ errors and relative deviations.

Standard	Section 1					Section 2					Section 3				
	n	Age (Ma)	2σ	MSWD	Deviation	*n*	Age (Ma)	2σ	MSWD	Deviation	*n*	Age (Ma)	2σ	MSWD	Deviation
GJ-1	26	608.1	2.3	1.1	0.02	20	608.9	3.1	0.65	0.15	15	608.8	3.1	0.72	0.13
Plešovice	16	337	2	1.5	0.05	19	337	1.9	1.4	0.05	15	337.2	1.5	0.79	0.01
91500	11	1066	4.9	0.87	0.09	21	1066	4.4	0.95	0.09	16	1069	4.5	0.64	0.37
BB9	15	560	3.3	1.4	0.19	13	559	2.8	0.68	0.37	6	566	5.7	1.5	0.87
M127	14	525	2.9	1.04	0.12	19	522	3.4	1.7	0.44	6	528	5.2	1.3	0.69
Standard	Section 4					Section 5					Section 6				
	n	Age (Ma)	2σ	MSWD	Deviation	*n*	Age (Ma)	2σ	MSWD	Deviation	*n*	Age (Ma)	2σ	MSWD	Deviation
GJ-1	20	607.5	3.3	1.5	0.08	11	607.8	3.5	0.36	0.03	37	608.6	2.4	1.6	0.10
Plešovice	18	337.6	2	1.7	0.12	24	338	1.5	1.1	0.24	9	338	3.4	2	0.24
91500	12	1070	6	1.3	0.46	15	1062	5.1	1.04	0.28	9	1068	6.0	1.4	0.28
BB9	4	559	8.1	2.7	0.37	5	564	7.7	2.1	0.51	16	558	3.2	1.6	0.55
M127	52	526	1.6	1.2	0.31	7	523	4.3	0.63	0.25	11	520	4.4	1.5	0.82
Standard	Section 7					Section 8					Section 9				
	n	Age (Ma)	2σ	MSWD	Deviation	*n*	Age (Ma)	2σ	MSWD	Deviation	*n*	Idade (Ma)	2σ	MSWD	Deviation
GJ-1	12	608.3	3.5	0.99	0.05	25	608.5	3.1	1.7	0.08	20	609.1	2.6	0.63	0.18
Plešovice	10	338.2	2	0.57	0.3	9	338	3.2	1.8	0.25	19	339	2.2	1.5	0.54
91500	8	1070	6.5	0.83	0.46	8	1064	11	1.9	0.09	6	1067	6.7	0.27	0.18
BB9		–	–	–	–		–	–	–	–		–	–	–	–
M127	24	528	3.1	1.7	0.69	9	528	3.2	0.54	0.69	9	523	3.3	0.25	0.25
Standard	Section 10					Section 11					Section 12				
	n	Age (Ma)	2σ	MSWD	Deviation	*n*	Age (Ma)	2σ	MSWD	Deviation	*n*	Age (Ma)	2σ	MSWD	Deviation
GJ-1	19	610	2.7	0.64	0.16	35	609.5	2.6	1.5	0.25	15	609.6	3.1	0.6	0.26
Plešovice	10	339	2.1	1.05	0.54	11	338.5	2.5	0.98	0.39	10	337.5	2.2	1.3	0.09
91500	6	1064	8.2	0.5	0.09		–	–	–	–		–	–	–	–
BB9		–	–	–	–		–	–	–	–		–	–	–	–
M127	9	524	3.4	0.55	0.06	8	524	5.4	2.2	0.06	9	528	4.5	1.8	0.69
Standard	Section 13					Section 14					Section 15				
	n	Age (Ma)	2σ	MSWD	Deviation	*n*	Age (Ma)	2σ	MSWD	Deviation	*n*	Age (Ma)	2σ	MSWD	Deviation
GJ-1	16	609.7	2.8	1.5	0.28	24	609.5	2.7	1.17	0.25	11	607	4	1.2	0.16
Plešovice	30	340	1.5	1.3	0.83	22	339.4	2.3	1.4	0.66	14	339	2.4	1.6	0.54
91500		–	–	–	–		–	–	–	–		–	–	–	–
BB9		–	–	–	–		–	–	–	–		–	–	–	–
M127	9	523	4.3	0.45	0.25		–	–	–	–		–	–	–	–
Standard	Section 16					Section 17					Section 18				
	n	Age (Ma)	2σ	MSWD	Deviation	*n*	Age (Ma)	2σ	MSWD	Deviation	*n*	Age (Ma)	2σ	MSWD	Deviation
GJ-1	24	609.5	2.7	1.17	0.19	18	609	3.4	1.5	0.16	18	609.5	3.7	1.8	0.26
Plešovice	14	338	2.6	1.8	0.24	9	337	2.2	1.06	0.05	13	338	2.5	1.6	0.25
91500		–	–	–	–		–	–	–	–		–	–	–	–
BB9		–	–	–	–		–	–	–	–		–	–	–	–
M127		–	–	–	–		–	–	–	–		–	–	–	–
Standard	Section 19					Section 20									
	n	Age (Ma)	2σ	MSWD	Deviation	*n*	Age (Ma)	2σ	MSWD	Deviation					
GJ-1	10	608	3.8	1.2	0	17	610.1	3.8	0.42	0.35					
Plešovice	9	338	2.1	0.34	0.24	8	338.9	2.6	0.97	0.51					
91500		–	–	–	–		–	–	–	–					
BB9		–	–	–	–		–	–	–	–					
M127		–	–	–	–		–	–	–	–					

MSWD: Mean Squares of the Weighted Deviation.
2σ: Analytical error.
n: Number of Analysis.

Zircons from the Alto Maranhão pluton are pink, euhedral and had conspicuous colors. They gave a TIMS age of 2124 ± 1 Ma (Noce et al., 1998). In this study, we obtained an upper intercept age of 2119 ± 18 Ma, with lower intercept at 591 ± 800 Ma (MSDW = 0.084) (Fig. 5e). Average mean ages from the ratios were 2111 ± 17 Ma ($^{207}Pb/^{206}Pb$), 2077 ± 16 Ma ($^{206}Pb/^{238}U$) and 2094.2 ± 9.1 Ma ($^{207}Pb/^{235}U$).

Zircons from the Poços de Caldas Complex phonolite are mm-to cm-wide, and are red to yellow translucent crystals (Fig. 3d). Thirty-three analyses on 12 of these grains gave concordant points with similar $^{206}Pb/^{238}U$ apparent ages in the range of 80–91 Ma. These points gave $^{206}Pb/^{238}U$ and $^{207}Pb/^{235}U$ weighted mean ages of 84.6 ± 1 Ma and 84.8 ± 1 Ma respectively, whereas a Concordia age of 84.4 ± 1 Ma was given by 23 of the 33 points (Fig. 5f). Identical but more conservative ages of 85 ± 2.8 (0.03% RSD) Ma and 86 ± 3.1 (0.04% RSD) Ma were calculated by averaging the $^{206}Pb/^{238}U$ and $^{207}Pb/^{235}U$ apparent ages. All the ages overlap within error and we assume the conservative age of 85 ± 2.8 Ma as the best

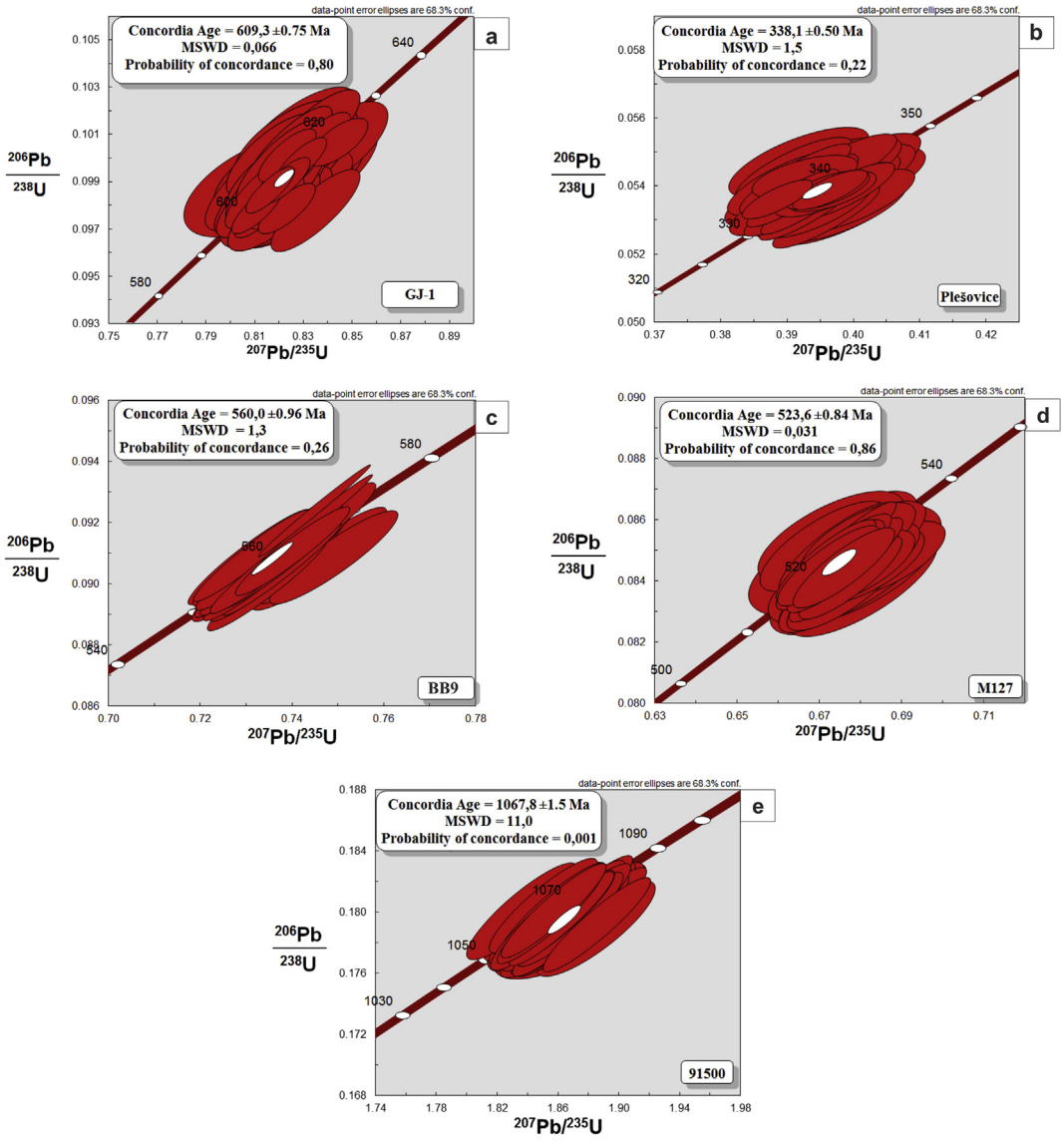

Fig. 4. Concordia ages for zircon standards (a) GJ-1 (b) Plešovice (c) BB9 (d) M127 and (e) 91500. As in Fig. 4 the cumulative effect of the large number of points resulted in statistically overestimated errors on the calculated ages. These errors should not be more accurate than the external reproducibility of the analysis (see text and Table 3 for details). The diagrams were generated in Isoplot (Ludwig, 2001).

approximation of the crystallization age of the hydrothermal veins that crosscut the phonolites and tinguaites in the western part of the PC complex.

5. Discussion

Optimization tests using a 213 UV Laser Ablation system coupled to an Agilent 7700x ICP-MS showed a significant improvement in sensitivity and reproducibility after a series of tests under varied conditions, including gas flow, laser beam diameter, laser energy and ablation time. Analysis with 40 μm beam seems the most suitable for low resolutions systems such as Quadrupole ICP-MS. We noted that a longer dwell time of 40 ms for ^{207}Pb mass can sometimes improve counts and drastically improve precision on the $^{207}Pb/^{206}Pb$ ratios (Table 2) and ages of Late-Proterozoic and Archean zircons. With a 30 μm beam (condition A), the counts are lower but satisfactory; this is verified by similar age reproducibility observed for conditions A and B (Table 2). Expanding the beam diameter to 50 μm increases the amount of sampled material but compromises the spatial resolution and therefore may not be suitable for complex zircons.

Changing ablation time from 40 s to 50 s improved slightly the counts, but fractionation increased. Long periods of ablation translated to deeper craters and again loss of spatial resolution deep into the crystals. Thus, the crater depth/diameter ratio is an essential factor for the optimization of quadrupoles, and it is directly related to the effect of elemental splitting, differential transport of U and Pb masses during ablation. Increasing this ratio causes the fractionation of elements, which results in undesirable age data. When reducing the usual frequency of 10 Hz–5 Hz, regardless of the diameter of the hole, the analytical error becomes extremely high due to low counts. Even increasing the ablation time from 40 s to 50 s, with the aim of supplying the least amount of material, the laser still does not supply a sufficient quantity of material to generate satisfactory counts. The analysis performed under these conditions provides a very unstable analytical signal and also very high errors. Thus, our preferable conditions are 30 μm, 10 Hz and 40 s of ablation time for Proterozoic zircons and

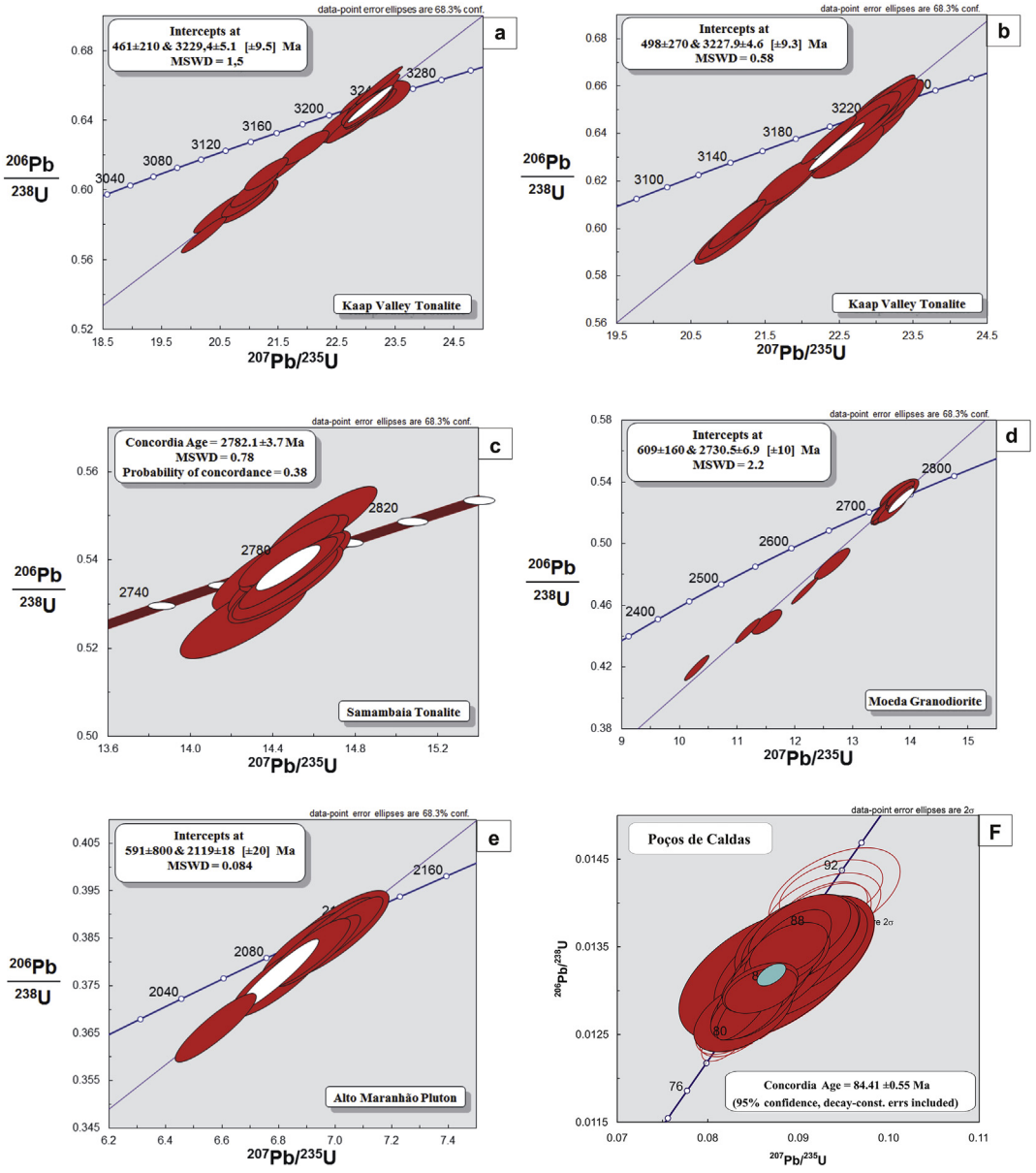

Fig. 5. Concordia diagrams for granitoide zircons: (a) and (b) for Kaap Valley Tonalite, (c) Samambaia Tonalite, (d) Moeda Granodiorite and (e) Alto Maranhão Pluton. f) Concordia diagram for several grains ($n = 23$) of the Poços de Caldas hydrothermal zircons.

40 μm, 10 Hz and 40 s of ablation time for Archean zircons (depending on the zircon internal complexity).

The signal stability is directly linked to the homogeneity of the gas mixture (He + Ar) and to the material removed by the laser. Compared to the previously used single tube, the Squid increased efficiency by decreasing the dispersion of the spectra. The use of the low-volume sample cell significantly increased the sensitivity of the signal obtained during the analysis and improved accuracy. There was a significant reduction in the washing time and a substantial increase in the rise time of the signal at the beginning of the tests, which in turn reduced the total time spent by the apparatus during the analysis and allowed a greater number of analyses to be conducted daily.

The long term results (using the same conditions) gave adequate reproducibility and acceptable errors. For instance, the GJ-1 zircon gave Concordia age values between 607 ± 4 Ma and 610.1 ± 3.8 Ma, 2σ uncertainties of 2–4%, relative deviations of 0.0–0.4%. For zircon Plešovice we obtained ages ranging from 337 ± 1.6 Ma to 340 ± 1.3 Ma (2σ uncertainties from 1.5 to 2.5%, relative deviations 0.02–0.35%) and uncertainties related with the mean ratios of 1.5–4%. The standard BB9 zircon generated Concordia from 558 ± 2.4 Ma to 566 ± 4.2 Ma, with 2σ uncertainties of 2.4–4.7%, relative deviations from 0.19 to 0.87% and uncertainties regarding the means of the ratios from 2.7 to 14%. The standard M127 zircon provided Concordia ages of 520 ± 3.5 Ma to 528 ± 3.4 Ma, 2σ uncertainties of 1.4–4.3%, relative deviations 0.06–0.82%, and uncertainties regarding the means of the ratios between 1.4 and 12%. Finally, zircon 91500 provided a minimum Concordia age of 1062 ± 5.1 Ma and a maximum value of 1070 ± 6.7 Ma, 2σ uncertainties of 4.4–8.2%, relative deviations 0.09–0.46%, and uncertainties of averaged ratios of 8.9–5%.

The method was also successful with older, more complex zircons, from granitoids of a range of ages. For example, for the Kaap Valley tonalite we obtained an upper intercept age of 3227 ± 3 Ma

and lower intercept age of 447 ± 150 Ma and concordant ages of 3218.3 ± 3.5 Ma to 3227 ± 3.7 Ma for two runs. This is identical, within error, to the U–Pb ages obtained by TIMS and SHRIMP techniques (3226 ± 14 Ma by Armstrong et al., 1990; 3229 ± 5 Ma by Tegtmeyer and Kroner, 1987; 3227 ± 1 Ma by Kamo and Davis, 1994). For the Samambaia tonalite (São Francisco Craton), we have obtained a Concordia age of 2782.1 ± 3.7 Ma, identical to the 2780 ± 3 Ma U–Pb TIMS age of Carneiro (1992). For the Moeda Granodiorite we obtained an upper intercept age of 2730.5 ± 6.9 Ma and a lower intercept age of 609 ± 160 Ma and Concordia age of 2728 ± 3.3 Ma identical to the 2730 ± 7 Ma U–Pb TIMS age of Machado et al. (1992). Finally, the Alto Maranhão Pluton gave an intercept age of 2119 ± 18 Ma (and lower intercept of 591 ± 800 Ma), slightly divergent but within error of the TIMS age of 2124 ± 1 obtained by Noce et al. (1998).

5.1. U–Th mineralization in the Poços de Caldas alkaline complex

The Poços de Caldas is considered the largest known alkaline complex of South America and one of the largest in the world (Woolley, 1987). According to Schorscher and Shea (1992), the petrographic associations of the PC alkaline rocks are potassium-rich phonolites and nepheline syenites, consisting broadly of K-feldspar, nepheline, sodic pyroxene and accessory minerals. The complex is marked by large deposits of U, Th and rare-earth elements (REEs) (Schorscher and Shea, 1992) in the form of bauxite, clays, zircon, caldasite, U–Zr–Mo, F and Th-REE (-Fe). Many of these deposits were caused by a late-stage alkaline fluid alteration (Frayha, 1962; Wedow, 1967; Gorsky and Gorsky, 1974; Putzer, 1976; Santos, 1976; Magno, 1985; Fraenkel et al., 1985; Ulbrich and Ulbrich, 1992).

Despite the number of age data accumulated for the PC complex over the last 60 years, there is still a strong disagreement about the emplacement age. Previously studies have pointed out a critical spread in the obtained ages from 54 Ma to 91 Ma (Ulbrich et al., 2002) which in turn cannot be included within one magmatic evolution of an alkaline complex. For instance, whole-rock Rb/Sr isochrons (Kawashita et al., 1984) gave ages of 89.8 ± 2.8 Ma (initial $^{87}Sr/^{86}Sr$ ratio of 0.7050 ± 1) from nepheline syenites and 86.3 ± 6.0 Ma (i.r., 0.7052 ± 1) from lujavrites and khibinites. Other Rb–Sr isochrons based on whole-rock samples of a nepheline syenite yielded an age of 74.2 ± 6.3 Ma (i.r. of 0.70511 ± 1) (Shea, 1992). K–Ar dating of a number of samples gave a substantially large spread in ages ranging from 89.3 to 54.2 Ma (see review in Ulbrich et al., 2002). The variances between the age dating methods may reflect differences in either emplacement ages, cooling of the rock massif and subsequent fluid-flow alteration. A key problem relates to late-stage fluid-host rock interactions. Fluid circulation particularly affects the K–Ar and Rb–Sr systems and therefore the accuracy of the published ages may be compromised by isotopic disturbance. According to Ulbrich et al. (2002) alteration may have added H_2O and K to the rocks, and leached out mainly Ca and Mg. Loss of radiogenic Ar is also expected to occur during leaching with the result that the whole rock and K-feldspar ages may be too young. To date, no previous study has attempted to constrain U–Pb ages for the mineralization in the complex.

The U–Pb method is insensitive to chemical alteration and is thus more adequate to constrain the emplacement age of the complex and the timing of fluid circulation. Textures of these rocks are essentially volcanic and suggest that the emplacement should have taken place within a period of a few million years. Our LA-Q-ICP-MS U–Pb zircon age of 85 ± 3 Ma for the zircon-filed cavities and veins in the western part of the PC complex is consistent with most of the older ages (>80 Ma) from whole rock Rb–Sr and some K–Ar in minerals such as biotite (Kawashita et al., 1984; Ulbrich et al., 2002). Our U–Pb age is also within error of the U–Pb (76 ± 12 Ma to 82 ± 11 Ma) ages produced from thorite crystals. These ages indicate that the zircon mineralization took place immediately after the emplacement of the volcanic body of the complex. According to previous studies, fluid alteration and associated mineralization in the PC complex can be compared to those of porphyry copper deposits in granites. The mineralization seems to be a result of both shattering of country rocks followed by extreme boiling fluid circulation in and above the roofs of crystallizing magma chambers. This is followed by cooling through the circulation of hydrothermal cells, mainly composed of supercritical water-rich solutions (*e.g.*, Burnham, 1979; Garda, 1990; Ulbrich and Ulbrich, 1992; Sawkins, 1990). Our U–Pb age is likely to reflect the age of the fluid circulation shortly after the emplacement of the phonolites. The overlapping ages are also consistent with relatively fast cooling shortly after emplacement. Given the regional extent of the host rock, encompassing much of the central and western part of the circular pipe, it is likely that much of the PC alkaline complex was emplaced shortly before 85 ± 3 Ma ago.

Acknowledgments

We acknowledge financial support from FAPEMIG (grant numbers RDP0067-10, RDP 00063-10, APQ03943) and PROPP/UFOP, grant 03/2014.

Appendix A. Supplementary data

Supplementary data related to this article can be found at http://dx.doi.org/10.1016/j.jsames.2015.04.007

References

Anhaeusser, C.R., Robb, L.J., 1983. Geological and geochemical characteristics of the Heerenveen and Mpuluzi batholiths south of the Barberton greenstone belt and preliminary thoughts on their petrogenesis. In: Special Publication of the Geological Society of South Africa, vol. 9, pp. 131–151.

Armstrong, R.A., Compston, M.J.W., Williams, I.S., 1990. The stratigraphy of the 3.5-3.2 Ga Barberton greenstone belt revisited: a zircon ion microprobe study. Earth Planet. Sci. Lett. 101, 90–106.

Bleiner, D., Günther, D., 2001. Theoretical description and experimental observation of aerosol transport processes in laser ablation inductively coupled plasma mass spectrometry. J. Anal. Atom. Spectr. 16, 449–456.

Burnham, C.W., 1979. Magmas and hydrothermal fluids. In: Barnes, H.L. (Ed.), Geochemistry of Hydrothermal Ore Deposits, second ed. Wiley, pp. 71–136.

Carneiro, M.A., 1992. O Complexo Metamórfico Bonfim Setentrional (Quadrilátero Ferrífero, Minas Gerais): Litoestratigrafia e evolução geológica de um segmento de crosta continental do Arqueano. University of São Paulo, Brazil. Unpublished PhD thesis, 233 p.

Darlin, J., Storey, Craig, Hawkesworth, C., Lightfoot, P., 2012. In-situ Pb isotope analysis of Fe–Ni–Cu sulphides by laser ablation multi-collector ICPMS: new insights into ore formation in the Sudbury impact melt sheet. Geochim. Cosmochim. Acta 99, 1–17. http://dx.doi.org/10.1016/j.gca.2012.09.028.

Elhlou, S., Belousova, E., Griffin, W.L., Pearson, N.J., O'reilly, S.Y., 2006. Trace element and isotopic composition of GJ red zircon standard by laser ablation. Geochim. Cosmochim. Acta 70, 158.

Ellert, R., 1959. Contribuição geológica do maciço alcalino de Poços de Caldas. Boletim de Faculdades de Filosófica, Ciência e Letras, University of São Paulo 237. Geologia 18, 1–64.

Fraenkel, M.O., Santos, R.C., Lourenço, F.E.V.L., Muniz, W.S., 1985. In: DNPM (Ed.), Jazida de urânio no planalto de Poços de Caldas, Minas Gerais. Principais Depósitos Minerais do Brasil, Brasil, pp. 89–103.

Frayha, R., 1962. Urânio e Tório no Planalto de Poços de Caldas. DNPM, 7p. (Boletim 116).

Fryer, B.J., Jackson, S.E., Longerich, H.P., 1993. The application of laser ablation microprobe-inductively coupled plasma-mass spectrometry (LAM-ICP-MS) to in situ (U)-Pb geochronology. Chem. Geol. 109, 1–8.

Garda, G.M., 1990. A alteração hidrotermal no contexto da evolução geológica do maciço alcalino de Poços de Caldas, MG - SP. Universidade de São Paulo, São Paulo. Dissertação de Mestrado, 213p.

Gorsky, V.A., Gorsky, E., 1974. Contribuição à mineralogia e petrografia do planalto de Poços de Caldas. Comissão Nacional de Energia Nuclear (CNEN), 93p. (Boletim 13).

Hinton, R.W., Upton, B.G.J., 1991. The chemistry of zircon: variations within and between large crystals from syenite and alkali basalt xenoliths. Geochim. Cosmochim. Acta 55, 3287–3302.
Horstwood, M.S.A., Foster, G.L., Parrish, R.R., Noble, S.R., Nowell, G.M., 2003. Common-Pb corrected in situ U–Pb accessory mineral geochronology by LA-MC-ICP-MS. J. Anal. Atom. Spectr. 18, 837–846.
Jackson, S.E., Pearson, N.J., Griffin, W.L., Belousova, E.A., 2004. The application of laser ablation-inductively coupled plasma-mass spectrometry to in situ U–Pb zircon geochronology. Chem. Geol. 211, 47–69.
Jeffries, T.E., Fernández Suárez, J., Corfu, F., Gutiérrez Alonso, G., 2003. Advances in U-Pb geochronology using frequency quintupled Nd:YAG based laser ablation system (lambda = 213nm) and quadrupole based ICP-MS. J. Anal. Atom. Spectrom. 18, 847–855.
Jeffries, T.E., Jackson, S.E., Longerich, H.P., 1998. Application of a frequency quintupled Nd:YAG source ($\lambda = 213$ nm) for laser ablation inductively coupled plasma mass spectrometric analysis of minerals. J. Anal. Atom. Spectrosc. 13, 935–940.
Kamo, S.L., Davis, D.W., 1994. Reassesment of Archean crustal development in the Barberton Mountain Land, South Africa, based on U–Pb dating. Tectonics 13, 167–192.
Kawashita, K., Mahiques, M.M., Ulbirich, H.H.G.J., 1984. Idades Rb/Sr de nefelina sienitos do anel norte do Maciço Alcalino de Poços de Caldas, MG-SP. In: Congresso Brasileiro de Geologia, vol. 23, pp. 244–245. Salvador, Anais.
Kinny, P.D., Compston, W., Williams, I.S., 1991. A reconnaissance ion-probe study of hafnium isotopes in zircons. Geochim. Cosmochim. Acta 55, 849–859.
Lana, C., Kisters, A., Stevens, G., 2010a. Exhumation of Mesoarchean TTG gneisses from the middle crust: Insights from the Steynsdorp core complex, Barberton granitoid-greenstone terrain, South Africa. Geol. Soc. Am. Bull. 122, 183–197.
Lana, C., Tohver, E., Cawood, P., 2010b. Quantifying rates of dome-and-keel formation in the Barberton granitoid-greenstone belt, South Africa. Precambr. Res. 177, 199–211.
Lana, C., Alkmim, F.F., Armstrong, R., Scholz, R., Romano, R., Nalini, H.A., 2013. The ancestry and magmatic evolution of Archaean TTG rocks of the Quadrilátero Ferrífero province, southeast Brazil. Precambr. Res. 230, 1–30.
Ludwig, K.R., 2001. Isoplot v.2.2-A Geochronological Toolkit for Microsoft Excel. Berkeley Geochronology Center, 53p. (Special Publication 1).
Machado, N., Noce, C.M., Ladeira, E.A., Belo, O.A., 1992. U–Pb geochronology of Archean magmatism and proterozoic metamorphism in the Quadrilátero Ferrífero, Southern São Francisco Craton, Brazil. Geol. Soc. Am. Bull. 104, 1221–1227.
Machado, N., Valladares, C., Heilbron, M., Valeriano, C., 1996. U-Pb geochronology of the central Ribeira Belt (Brazil) and implications for the evolution of the Brazilian Orogeny. Precambr. Res. 79, 347–361.
Magno Jr., L.B., 1985. The alkaline district of Poços de Caldas. Poços de Caldas, Nuclebras CIPC internal publication, 15p.
Nasdala, L., 2007. TIMS Table with U-Pb Concordia Ages for M127 Standard. Personal communication.
Nasdala, L., Hofmeister, W., Norberg, N., Martinson, J.M., Corfu, F., Dörr, W., Kamo, S.L., Kennedy, A.K., Kronz, A., Reiners, P.W., Frei, D., Kosler, J., Wan, Y., Götze, J., Häger, T., Kröner, A., Valley, J.W., 2008. Zircon M257-a homogeneous natural reference material for the ion microprobe U-Pb analysis of zircon. Geostand. Geoanal. Res. 32, 247–265.
Noce, C.M., Machado, N., Teixeira, W., 1998. U–Pb geochronology of gneisses and granitoids in the Quadrilátero Ferrífero (southern São Francisco craton): age constraints for Archean and Paleoproterozoic magmatism and metamorphism. Rev. Bras. Geociên. 28, 95–102.
Putzer, H., 1976. Metallogenetische Provinzen in Suedamerika. Schweizerbart'sche, Stuttgart, 316p.
Robb, L.J., Anhaeusser, C.R., Van Nierop, D.A., 1983. The recognition of the Nelspruit batholith north of the Barberton greenstone belt and its significance in terms of Archaean crustal evolution. In: Special Publication of the Geological Society of South Africa, vol. 9, pp. 117–130.
Romano, R., Lana, C., Alkmim, F.F., Stevens, G.S., Armstrong, R., 2013. Stabilization of the southern portion of the São Francisco Craton, SE Brazil, through a long-lived period of potassic magmatism. Precambr. Res. 224, 143–159.
Rubato, D., 2001. Zircon trace element geochemistry: partitioning with garnet and the link between U–Pb ages and metamorphism. Chem. Geol. 184 (1), 123–138.
Santos, R., 1976. Geology and Mining Development of the C-09 Uranium Deposit. LAEA, 28p. (Bulletin 162).
Santos, M.M., Lana, C.C., Cipriano, R.A.S., 2014. Development of zircon standards for U-Pb geochronology by laser ablation. In: South-American Symposium on Isotope Geology, vol. 9, p. 296. São Paulo.
Sarkar, Chiranjeeb, Storey, Craig, Hawkesworth, Chris J., 2014. Using perovskite to determine the pre-shallow level contamination magma characteristics of kimberlite. Chem. Geol. 363, 76–90. http://dx.doi.org/10.1016/j.chemgeo.2013.10.032.
Sawkins, F.J., 1990. The Olympic Dam Cu-U-Au Deposit, south Australia. In: Minerals, Rocks, Ando Mountains Metal Deposits in Relation to Plate Tectonic, second ed., vol. 17. Springer, Berlin, pp. 261–264.
Schorscher, H.D., Shea, M.E., 1992. The regional geology of the Poços de Caldas alkaline complex: mineralogy and geochemistry of selected nepheline syenites and phonolites. J. Geochem. Explor. 45, 25–51.
Shea, M.E., 1992. Isotopic geochemical characterization of selected nepheline syenites and phonolites from the Poços de Caldas alkaline complex, Minas Gerais, Brazil. J. Geochem. Explor. 45, 25–51.
Sláma, J., Košler, J., Condon, D.J., Crowley, J.L., Gerdes, A., Hanchar, J.M., Horstwood, M.S.A., Morris, G.A., Nasdala, L., Norberg, N., Schaltegger, U., Schoene, B., Tubrett, M.N., Whitehouse, M.J., 2008. Plešovice zircon – a new natural reference material for U–Pb and Hf isotopic microanalysis. Chem. Geol. 249, 1–35.
Stacey, J.S., Kramers, J.D., 1975. Approximation of terrestrial lead isotope evolution by a two-stage model. Earth Planet. Sci. Lett. 26, 207–221.
Storey, C.D., Jeffries, T.E., Smith, M., 2006. Common Pb-corrected laser ablation ICP-MS U-Pb systematics and geochronology of titanite. Chem. Geol. 227, 37–52.
Tegtmeyer, A.P., Kroner, A., 1987. U-Pb zircon ages bearing on the nature of early Archean greenstone belt evolution, Barberton Mountain Land, Southern Africa. Precambr. Res. 36, 1–20.
Thirlwall, M.F., Walder, A.J., 1995. In-situ hafnium isotope ratio analysis of zircon by inductively coupled plasma multiple collector mass spectrometry. Chem. Geol. 122, 241–247.
Ulbrich, H.H., Ulbrich, M.N.C., 1992. O Maciço Alcalino de Poços de Caldas, MG-SP: características petrográficas e estruturais. In: Congresso Brasileiro de Geologia, 37. São Paulo, Anais, Roteiro de Excursões 5: 64p.
Ulbrich, H.H.G.J., Vlach, S.R.F., Ulbrich, M.N.C., Kawashita, K., 2002. Pene-contemporaneous syenitic-phonolitic and basic-ultrabasic-carbonatitic rocks at the Poços de Caldas alkaline massif, SE, Brazil: geologic and geochronologic evidence. Rev. Bras. Geociênc. 32, 15–26.
Van Achterbergh, E., Ryan, C.G., Jackson, S.E., Griffin, W.L., 2001. Data Reduction Software for LA-ICP-MS: Appendix. Association Canada (MAC), Canada, 239p. (Short Course Series 29).
Wedow Jr., H., 1967. The Morro do Ferro thorium and rare earth are deposits, Poços de Caldas District. U.S. Geological Survey, Brazil. USA, 34p. (Bulletin, 1185-D).
Wiedenbeck, M., Allé, P., Corfu, F., Griffin, W.L., Meier, M., Oberli, F., Von Quadt, A., Roddick, J.C., Spiegel, W., 1995. Three natural zircon standards for U–Th–Pb, Lu–Hf, trace element and REE analysis. Geostand. Newsl. 19, 1–23.
Woolley, A.R., 1987. Alkaline Rocks and Carbonatites of the World. Part 1. North and South America. University of Texas Press, London, 216p.